Contributions of cryptochromes and phototropins to stomatal opening through the day

Wang, Fang

2020-02-12

Wang , F , Robson , T M , Casal , J J & Aphalo , P J 2020 , ' Contributions of cryptochromes and phototropins to stomatal opening through the day ' , Functional Plant Biology , vol. 47 , no. 3 , pp. 226-238 . https://doi.org/10.1071/FP19053

http://hdl.handle.net/10138/313709
https://doi.org/10.1071/FP19053

unspecified
acceptedVersion

Title Page

Title: Contributions of cryptochromes and phototropins to stomatal opening through the day

Authors: Fang Wang [1], T. Matthew Robson [1], Jorge J. Casal [2,3], Alexey Shapiguzov [1,4], Pedro J. Aphalo [1*]

1. Viikki Plant Science Centre (ViPS), Department of Biosciences, Faculty of Biological and Environmental Sciences, University of Helsinki, 00014, Finland
2. IFEVA, Facultad de Agronomía, Universidad de Buenos Aires and CONICET, Av. San Martín 4453, 1417 Buenos Aires, Argentina
3. Fundación Instituto Leloir, Instituto de Investigaciones Bioquímicas de Buenos Aires–CONICET, 1405 Buenos Aires, Argentina
4. Permanent address: Institute of Plant Physiology, Russian Academy of Sciences, Botanicheskaya Street, 35, 127276 Moscow, Russia

* Corresponding author: pedro.aphalo@helsinki.fi

Summary (80/80 words)

We studied the times of day at which cryptochromes and phototropins participate in stomatal responses to light, by subjecting *Arabidopsis* mutants in these two photoreceptors to 11-hour exposure to blue-, red- or green-light. Under blue light, phototropins had relatively greater importance at the start of the photoperiod, whereas cryptochromes were important for stomatal opening throughout the photoperiod. This different timing of contributions by two families of photoreceptors to stomatal opening indicates that the mechanism is more complicated than usually assumed.

Abstract (196/200 words)

The UV-A/blue photoreceptors phototropins and cryptochromes are both known to contribute to stomatal opening (Δg_s) in blue light. However, their relative contributions to maintenance of g_s in blue light through the whole photoperiod remains unknown. To elucidate this question, *Arabidopsis phot1 phot2* and *cry1 cry2* mutants (MTs) and their respective wild types (WTs) were irradiated with 200 μmol m^{-2} s^{-1} of blue-, green- or red-light (BL, GL or RL) throughout a 11-hour photoperiod. Stomatal conductance (g_s) was higher under BL, than under RL or GL. Under RL, g_s was not affected by either of the photoreceptor mutations, but under GL g_s was slightly lower in *cry1 cry2* than its WT. Under BL, the presence of phototropins was essential for rapid stomatal opening at the beginning of the photoperiod, while maximal stomatal opening beyond 3 h of irradiation required both phototropins and cryptochromes. Time courses of whole-plant net carbon assimilation rate (A_{net}) and the effective quantum yield of photosystem II photochemistry (ΦPSII) were consistent with an A_{net}-independent contribution of BL on g_s both in *phot1 phot2* and *cry1 cry2* mutants. The changing roles of phototropins and cryptochromes through the day may allow more flexible coordination between g_s and A_{net}.

Keywords (max 10)

Arabidopsis thaliana; blue light; diurnal pattern; gas exchange; green light; photosynthesis; red light; stomata;

Introduction

The major function of leaf stomata is to open for photosynthetic carbon fixation and to close for the avoidance of dehydration. This function is a compromise, determined by internal as well as environmental factors and tightly related to the photosynthetic carbon metabolism (Cowan and Farquhar 1977). Light is the ultimate energy source for plant growth, and one of the most important environmental cues for stomatal opening. Indoor experiments have verified that different light qualities stimulate stomatal opening (Sharkey and Raschke 1981; Shimazaki *et al.* 2007). Blue light (BL) is the most effective band of the visible spectrum inducing stomatal opening even at irradiances as low as 1 $\mu mol\, m^{-2}\, s^{-1}$ and this BL-specific stomatal opening is considered as independent on photosynthesis (A_{net}) (Shimazaki *et al.* 2007), whereas stomatal opening driven by red light (RL) is thought to depend on photosynthetic metabolism (e.g. Sharkey and Raschke 1981; Wang *et al.* 2011). A well-documented link exists between net carbon assimilation rate in the mesophyll A_{net} and stomatal conductance (g_s) through depletion of CO_2 concentration in the leaf intercellular air spaces (C_i) by A_{net} and the opening response of stomata to a decrease in C_i (e.g. Aphalo and Jarvis 1993; Roelfsema *et al.* 2002). However, it has also been shown that C_i does not always fully explain stomatal opening under RL and the involvement of signals different from C_i has been suggested to also link g_s and A_{net} (reviewed by Lawson *et al.* 2010; Matthews *et al.* 2017). In addition, as stomata in epidermal peels open under RL in the absence of mesophyll, guard cell A_{net} may also contribute to stomatal opening (Matthews *et al.* 2017; Shimazaki *et al.* 2007). Like RL, BL also penetrates the epidermis and drives photosynthesis in the mesophyll. Thus, direct stomatal opening in response to BL perceived through photoreceptors and indirect photosynthetically driven opening are both involved in BL-induced stomatal opening when irradiance is not weak (Sharkey and Ogawa 1987). Compared with BL- and RL-induced responses, stomatal opening induced by green light (GL) has been studied less frequently, and findings have been inconsistent among studies. GL is generally considered to be less effective in opening stomata than RL, and much less effective than BL (Sharkey and Raschke 1981; Folta and Maruhnich 2007), and also able to reverse stomatal opening induced by BL under a background of RL (Frechilla *et al.* 2000; Talbott *et al.* 2002).

Cryptochromes (crys) and phototropins (phots) are both flavoprotein photoreceptors with different protein structures activated by radiation spanning the ultraviolet-A (UVA) and BL (Banerjee and

Batschauer 2005; Christie *et al.* 2015). Both of crys and phots absorb *in vitro* mainly UV and BL when dark adapted, while, when light-adapted, crys but not phots strongly absorb GL in addition to UV and BL (Banerjee *et al.* 2007; Christie *et al.* 2015). Crys are known to be involved in the inhibition of hypocotyl elongation, entrainment of the circadian rhythm, stomatal opening and shade avoidance (Sellaro *et al.* 2010; Chen *et al.* 2012; Sellaro *et al.* 2012), while phots are implicated in the control of phototropism, chloroplast movement, leaf expansion and movement (Briggs and Huala 1999; Christie 2007). Certain roles in photomorphogenic processes have been attributed to crys and phots based on the comparison of gene expression, molecular pathways and biochemical functions that they promote (Briggs and Huala 1999; Liscum *et al.* 2003; Ohgishi *et al*. 2004). In the regulation of stomatal responses, phots seem to be dominant in rapid stomatal response to BL at a low fluence rate (Shimazaki *et al.* 2007; Chen *et al.* 2012), while crys regulate stomatal opening at relatively high irradiances of BL and also could affect g_s under background RL (Talbott *et al.* 2003; Boccalandro *et al.* 2012). Phots are reported to ultimately activate the plasma membrane H^+-ATPase that drives K^+ uptake leading to increased turgor pressure and stomatal opening (Inoue *et al.* 2010). Crys have been shown to interact with CONSTITUTIVE PHOTOMORPHOGENIC1 (COP1) (Shimazaki *et al.* 2007) in circadian-rhythm regulation (Briggs and Huala 1999). Kinoshita *et al.* (2011) found a possible link between phot-mediated stomatal responses to BL and the circadian clock through *FLOWERING LOCUS T* (FT), whereas Ando *et al.* (2013) using epidermal peels provide evidence for cry affecting stomatal opening through FT and the circadian clock.

Tenhunen *et al.* (1987) studied stomatal function by following daily patterns of gas exchange in various natural environments, concluding that the coupled relationship between g_s and A_{net} is important in leaf function over a diurnal period. Various studies have attempted to identify the underlying mechanism behind these diurnal patterns. Talbott and Zeiger (1996) explored a model of osmoregulation driving stomatal diurnal movements under white light (WL), since potassium ions (K^+) were found to be the predominant guard-cell osmoticum during the first half of the day and sugars (sucrose and malate) in the second half of the day. This model was extended by Tallman (2004) to incorporate regulation of diurnal stomatal movements by dual-source-controlled fluctuations in ABA metabolism. The dynamics of stomatal regulation in whole plants are poorly understood and Matthews *et al.* (2017) recommend that future research takes them into consideration. While crys and phots are known to induce stomatal opening (Chen *et al.* 2012), their

contribution towards the regulation of diurnal patterns of stomatal opening themselves, and through interaction with other established mechanisms of stomatal control, have not been elucidated. Here we aim to answer the following two questions:

a) Are diurnal patterns in g_s correlated with diurnal patterns in A_{net} under blue, green and red monochromatic light? Lack of correlation would imply that mechanisms independent of A_{net}, likely attributable to photoreceptors, make an important contribution to light-induced g_s through the photoperiod.
b) Are the roles of the BL photoreceptors crys and phots in stomatal opening different and do they vary during the photoperiod? Such differences would imply that these photoreceptors contribute to determining the shape of diurnal patterns of g_s.

To answer these questions, we concurrently measured the diurnal time courses of g_s, A_{net} and C_i in *Arabidopsis thaliana* double mutant types (MTs) *phot1 phot2* and *cry1 cry2* and their wild types (WTs) under constant irradiance of RL, GL or BL, or in darkness.

Material and Methods

Plant materials and growth conditions

Arabidopsis thaliana double MT *phot1-5 phot2-1* and its WT Columbia-5 (alias Col-0 *gl1-1*, glabrous derivative of Col-0, shortened to Col-5), and double MT *cry1-1 cry2-1* and its WT Landsberg *erecta* (L*er*) were employed in the experiments. For a given replicate, seeds of all genotypes were produced at the same time, by plants grown side-by-side. Seeds were sown in square plastic 70-×-70-mm pots filled with a substrate composed of 50% pre-fertilised-and-limed peat and 50% vermiculite. The sown pots were kept at 4 °C in darkness for two days and three nights, and then moved to a controlled-environment walk-in growth room.

After one week's growth, each single plant was transplanted into a pot (60 mm in diameter and 47 mm in height) into the same substrate as used for germination and continued to grow in a walk-in growth room for three weeks. Gas exchange measurements were made on these single seedlings. Given that only one plant could be measured per day, a cohort of plants was grown each week to produce a continuous supply of equivalent plants. For chlorophyll fluorescence measurements, seedlings were transplanted into trays of 3-×-2 cells. Each cell was 45-×-55 mm across and 60 mm

deep. A balanced design was used to arrange the genotypes in the trays, with different genotypes spatially interspersed and their positions randomised.

In the growth room, fluorescent tubes (L 58W/865 LUMILUX, OSRAM, Germany) supplied a constant photon irradiance of 205 ± 15 µmol m^{-2} s^{-1} PAR (mean ± s.e., see Fig. SI1 for spectra), with a 12 h photoperiod from 7.00 a.m. (ZT = 00:00, expressed in hours and minutes) to 7.00 p.m. Air relative humidity and air temperature, next to the growing plants, were recorded by three DS1923 Hygrochron temperature/humidity data loggers (iButtons, Maxim Integrated, San Jose, CA, U.S.A). Relative humidity (RH) was 67 ± 0.4% / 74 ± 0.5% (mean ± SE) day / night and temperature (T) was 22 ± 0.03 °C / 20 ± 0.05 °C (mean ± SE) day / night.

Gas exchange measurements

Light treatments

A custom-built light source based on three-colour LED arrays was used. The light source consisted of two RGB LED arrays (Red-Green-Blue 90 Die Hex type NHXRGB090S00S, Norlux, Chicago, USA) assembled on a 120×100×35 (L×W×H) mm passive heat sink. The spectral photon irradiance for the three channels is given in Fig. SI2A and the actual light-source is shown in Fig. SI2B. The gap between the top of the chamber and the light source 30-mm above was sealed with high-density black foam to block room-light from entering the chamber. The foam was covered on the inside by a high-reflectance-plastic white-reflection standard card (Zebra check card, Novoflex, Memmingen, Germany) to improve light-field evenness. The light source was powered by three programmable power supplies (GW INSTEK PSP-2010, New Taipei City, Taiwan China) in constant current mode. The current setting was adjusted to achieve an irradiance of 200 µmol m^{-2} s^{-1} measured with the built-in sensor of the gas-exchange chamber at the time when each plant was enclosed; irradiance remaining in all cases within ± 10% of the set value for the whole day. One power source was used to control each colour channel in both arrays. Each power supply was switched on at ZT = 00:00 (7 a.m.) and off at ZT = 11:30 (6.30 p.m.) by a program running on a computer. For the experiments reported here, only one single-colour channel was used at a time. The cuvette was darkened for the whole day in the darkness treatments by covering its top with the darkening plate provided as part of the gas-exchange system.

A portable gas exchange system GFS-3000 with Arabidopsis whole-plant Chamber 3010-A (GFS, Walz, Effeltrich, Germany) was used to measure transpiration, A_{net}, C_i and g_s. Settings were 750 µmol s^{-1} air flow rate, level 5 impeller speed, 390 ppm ambient CO_2 (C_a), 22 °C cuvette air temperature and 67% relative humidity. The average leaf temperature was stable before and during the light treatments at 21.69 °C – 21.86 °C (SI Script). The actual values of C_a accounting for any deviation from the set value are given in Table SI1. Plants were enclosed in the *Arabidopsis* cuvette for 22 to 23 h. Drift in ambient conditions and bias in measurements were avoided by regular IRGA re-zeroing. The chamber was under excess pressure, adjusted by means of its vent valve at the bottom of the pot compartment. This coupled with a collar of white polyethylene film covering the surface of the soil prevented soil respiration and evaporation from interfering with the measurement of shoot gas exchange.

The order in which treatments and genotypes were measured was fully randomized to avoid bias, including bias caused by the age differences between plants within the weekly cohorts. So as to ensure consistency, settings and the measurement protocol were stored as a program and ran uninterrupted for 22-23 h during each measurement session using the GFS-Win (Walz) program on a computer (different from the one for the light power supply). Each measurement cycle started with one IRGA re-zeroing, followed by acquisition of 4 data records and ended with another IRGA re-zeroing followed by an interval until the start of the next cycle, on a 33-36 min loop (SI Script). The measuring protocol consisted of enclosing a plant in the cuvette the previous evening at approximately 6:30 p.m. (ZT = -12:30), immediately after transfer from the growth room to an adjacent laboratory. The enclosed plant remained in darkness, under the conditions indicated above, until the next morning, when at 7 a.m. (ZT = 00:00) one of the colour channels of the light source was switched on (except in the darkness treatment). The data collected per plant at 147 or more time points between midnight (ZT = -07:00) and 6.30 p.m. (ZT = 11:30) were checked for any anomalies.

Delta stomatal conductance (Δg_s) was calculated as the difference between each g_s value measured during the photoperiod and g_s measured in darkness on the same plant at the last time-point before the start of the photoperiod. This calculated Δg_s allowed for more precise analysis of the differences between genotypes because it enabled a correction to be made for differences in baseline values of g_s in darkness among individual plants. The C_i was expressed as a fraction of

C_a. to minimize any effect of slight fluctuations in C_a (Table SI1). Raw g_s data are presented in Fig. SI3, A_{net} in Fig. SI4 and C_i/C_a in Fig. SI5.

Leaf area calculation

As whole plants were measured, calculation of gas-exchange rates expressed per unit area required the estimation of the enclosed illuminated leaf area. The projected rosette area was used as a proxy for the illuminated leaf area. The plant was taken from the growth room before the end of the photoperiod (*ca.* 6.30 p.m.) when leaves were horizontal in all genotypes. Next, as mentioned above, a collar of white polyethylene film was placed below the rosette covering the soil, providing a contrasting background for the photographs and subsequently photographed on a copy stand alongside an identical empty pot covered with a black square pattern drawn on a white background used as a reference (NIKON D100, AF NIKKOR 50MM f/1.8D, Japan). ImageJ (Schneider *et al.* 2012) was employed to estimate the whole rosette projected area (Wang 2017). The average projected rosette area of individual plants used for gas exchange measurements was 457 ± 2 mm^2 in WT Col-5, 413 ± 2 mm^2 in its MT *phot1 phot2*, 511 ± 3 mm^2 in WT L*er*, and 518 ± 2 mm^2 in its MT *cry1 cry2* (mean ± s.e.).

In a subset of plants of each genotype, the total area of all the leaves was measured in addition to the rosette area to assess overlap among leaves, given that the leaves were nearly horizontal when sampled during the photoperiod. All leaves were excised at the base of the petiole, leaf blades held flat to avoid curling, photographed and quantified in the same way as rosette projected area. The relationships between rosette projected area and the total leaf area estimates were: 88 ± 6 % in WT Col-5 and 62 ± 3 % in its MT *phot1 phot2*, 94 ± 2 % in WT L*er* and 90 ± 4 % in its MT *cry1 cry2* (mean ± s.e.).

Chlorophyll fluorescence measurements

IMAGING-PAM M-Series (Walz, Effeltrich, Germany) was employed to make chlorophyll fluorescence measurements. These were performed in a darkened purpose-built cubicle located within a large well-ventilated hall, with *c* 500 ppm C_a and *c* 30 % RH. Four plants of each of the four genotypes were measured simultaneously in one tray, each tray being a true replicate or block. The blue LED (450 nm, 230 µmol m^{-2} s^{-1}) built-into the IMAGING-PAM was kept on from 7.00 a.m. (ZT = 00:00) until 5.00 p.m. (ZT = 10:00). Irradiance was measured at the level of the

seedlings at the centre of the tray. The following protocol was used to obtain a diurnal time course of the effective quantum yield of photosystem II photochemistry (ΦPSII). Against the background of continuous actinic light (230 μmol m^{-2} s^{-1} above the rosette, measured with a LI-250A light meter – LI-COR, Lincoln, Nebraska, USA), the low-intensity measuring light was triggered once every two minutes throughout the experiment to probe steady-state fluorescence under illumination (F_s). Saturating light pulses (5000 μmol m^{-2} s^{-1}, duration of 1 s from an LED-Array Illumination Unit IMAG-MAX/L) were triggered once every 10 min to measure maximal fluorescence under illumination (F_m'). ΦPSII was calculated as $(F_m'-F_s)/F_m'$ (Genty *et al.*, 1989). The measuring light was of intensity 2 and frequency 1 set in Walz Imaging Win Software. The programmed protocol can be checked in SI Script.

Stomatal density and size

Two young fully-expanded leaves were collected from each of 10 plants per genotype grown under the same conditions as the plants used for gas exchange for the purpose of making comparisons of stomatal density and size. These two leaves were painted with clear nail varnish, one on the adaxial side and the other on the abaxial side. When almost dry, the nail-varnish imprints were peeled off the leaf with the aid of a piece of transparent sticky tape. The tape was cut so as to keep the peeled imprint and discard the rest. The imprint was transferred to a microscope slide and photographed under a microscope (LEICA DMLB 2500, Germany). Two fields of view were selected from each slide. There were no statistically significant differences among genotypes in the density of stomata (Table SI2: abaxial, p = 0.54; adaxial, p = 0.83) were counted on images taken at 10 × magnification (the image size was 879 μm × 659 μm), or stomatal sizes (Table SI2: abaxial, p = 0.95, adaxial, p = 0.60) measured in ImageJ on images at 20× magnification (the image size was 442 μm × 331 μm).

Optical properties of leaves

Leaf transmittance and absorptance was measured with a Jaz spectrometer from Ocean Optics (Dunedin, USA) with four modules, DPU module, PX Pulsed Xenon Light source module and two UV/VIS spectrometer modules, using a Spectroclip-TR probe consisting of two integrating spheres facing each other on opposite sides of the leaf. A white/black reflectance target was used to obtain a reference spectrum (Ocean Optics). The spectral reflectance and transmittance were both

measured at the same position on each of two leaves per plant, and used to estimate the spectral absorptance (fraction of radiation absorbed expressed per nanometre was calculated as 1.0 minus the sum of spectral reflectance and spectral transmittance). For each genotype, five replicates were measured. We calculated the fraction of light absorbed by each genotype under RL, GL and BL by multiplying the fractional spectral absorptance of the leaves by the light spectrum measured for each LED channel (Aphalo 2015). The mean leaf absorptance was computed for each combination of light channel and genotype based on the replicate estimates.

Data Analyses

Statistical analyses were done with R 3.2.0 (R Core Team 2016) within RStudio. Package mgcv (Wood 2006) was used for fitting additive mixed models (AMM) and package nlme (Pinheiro and Bates 2000) for fitting linear mixed effects (LME) models. The output of the R scripts used in the analysis and both final and intermediate results are contained in a script (SI Script).

Because of the complex shape of the daily course of Δg_s we chose an additive model to test for differences in the shape of the daily course among genotypes (Wood 2006). Additive models are routinely used in various fields of research when data along the *x*-axis are densely spaced and response-curve shapes are complex (e.g. de Dios *et al.* 2016 and Saw *et al.* 2017). An AMM was fitted to Δg_s values with time-of-day as a continuous explanatory variable and genotype as a factor. Each MT was compared with its corresponding WT. The AMM we fitted uses splines to describe the change with time: it is a mixed model because it includes random terms and grouping factors to describe the variability among plants. The model avoids pseudo-replication, as it takes each plant as a replicate, even though 68 measured values were acquired from each plant. When considering the shape of diurnal patterns of Δg_s in detail, our interpretation was based on differences between the fitted curves and the overlap (or not) of the $p = 0.95$ confidence bands, shown in the figures. Within each light treatment, overall differences between each MT and the corresponding WT were assessed by formal, ANOVA-like tests of significance. A critical *p* value of 0.05 for significance was used in these tests. We also used a more traditional approach fitting a third-order polynomial (with an intercept forced to zero at ZT = 00:00 because of the use of Δg_s values), in a linear mixed effects (LME) model, to analyse the time course during the first hour of the photoperiod and confirm the validity of the AMM analysis.

A second-order polynomial was fitted to C_i/C_a and first-order polynomials to A_{net} and ΦPSII, using LME models accounting for the repeated measures, as described above. Because of the steep increase in A_{net} and ΦPSII and decrease in C_i/C_a immediately after the light was turned on at ZT = 00:00, which cannot be fitted to our LME models, data from the first cycle of measurements (ZT = 00:00 to ZT = 00:30) were not included (SI Script).

Results

Diurnal patterns of Δg_s and respiration in darkness

Prior to the light treatments (ZT = 00:00), stomata were not completely closed in any genotype (g_s 159 ± 13 mmol m^{-2} s^{-1}, mean ± s.e. at ZT = 00:00). Nevertheless, during the last hour in the dark (ZT = -01:00 to ZT = 00:00), Δg_s remained almost constant, increasing by less than 5 % in all genotypes (SI Script).

In darkness, during what would otherwise be the normal photoperiod from ZT = 00:00 to ZT = 11:00, Δg_s in all genotypes slowly decreased as stomata continued to close from ZT = 00:00 onwards (Fig. 1a, b). The Δg_s of *phot1 phot2* was similar to its WT but in *cry1 cry2* Δg_s differed from its WT by the end of the day. In L*er* WT, Δg_s decreased by about 100 mmol m^{-2} s^{-1} during the photoperiod but in *cry1 cry2* it only decreased approximately 60 mmol m^{-2} s^{-1} over the same period (Fig. 1b).

In darkness, $A_{net,}$ was negative as a result of respiration, and was small in MTs and their respective WTs (Fig. 1c, d). The slopes, describing the change in A_{net} with time, did not differ between *cry1 cry2* and its WT (p = 0.90; Fig. 1d), but did between *phot1 phot2* and its WT ($p < 0.0001$, Fig. 1c).The respiration rate in *phot1 phot2* decreased from the beginning to the end of the photoperiod by 0.38 μmol m^{-2} s^{-1} (respiration rate range: 1.63 - 1.25 μmol m^{-2} s^{-1}), whereas in its WT, this decrease was only about 0.05 μmol m^{-2} s^{-1} (1.30 - 1.25 μmol m^{-2} s^{-1}) (Fig. 1c).

Diurnal patterns of Δg_s under BL, GL and RL

Fig. 2a shows the diurnal patterns of Δg_s under BL, GL and RL, as curves fitted using AMM and their 95% confidence bands. In WTs, RL, GL and BL all induced stomatal opening at equal photon irradiance of 200 μmol m^{-2} s^{-1}, but of these, BL was the most effective. Spectral measurements of leaves and LEDs and calculations based on them showed that in-spite of differences in leaf

absorptance in the green-red region (516 - 643 nm) the estimated total absorbed flux of BL photons was approximately 8% and 10% more than under RL or GL, respectively (Fig. SI6). Even though the absorptance of leaves of *cry1 cry2* was slightly lower in the green-red region than that of the other genotypes, the differences in absorbed photons between it and its L*er* WT was 3% or less under all light treatments (Fig. SI6a).

The maximum fitted Δg_s under BL was over 300 mmol m^{-2} s^{-1}, approximately three times that under GL or RL (Fig. 2). In L*er* WT, Δg_s was higher in GL than in RL from ZT = 01:30 to ZT = 06:00. In addition to the differences in maximal Δg_s, the shape of the time course was different under BL compared with GL or RL, in both L*er* WT and Col-5 WT (Fig. 2a, b). The time courses of g_s were consistent among replicate plants within treatments (Fig. SI3).

Under BL, the shapes of whole-day Δg_s time courses were strikingly different in the MTs compared to their corresponding WTs (Fig. 2a, b). In the WTs, Δg_s increased rapidly upon illumination at ZT = 00:00 and continued increasing, reaching 375 mmol m^{-2} s^{-1} (Col-5 WT) and 300 mmol m^{-2} s^{-1} (L*er* WT) at its maximum at ZT = 06:00 after which it started to decline. In the *phot1 phot2* mutant (Col-5 background), Δg_s initially increased more gradually, reaching a maximum that was only two thirds that of its WT, and later Δg_s decreased like in its WT (Fig. 2a, BL). In the *cry1 cry2* mutant (L*er* background), Δg_s was similar to that of its WT during the first 2 hours after the start of illumination, but later in the day the maximum Δg_s in *cry1 cry2* was only approximately half that of its WT, and likewise the decrease in Δg_s after ZT = 06:00 was smaller than in its WT (Fig. 2b, BL).

Under GL, the shape of the time course of Δg_s differed only between *cry1 cry2* and its WT and not between *phot1 phot2* and its WT (Fig. 2a, b). During the first hour of illumination (ZT = 00:00 to ZT = 01:00), Δg_s increased at a similar slow rate in all four genotypes (Fig. 5). From ZT = 02:00 to ZT = 06:00 Δg_s was 33% lower in *cry1 cry2* than in its WT (Fig. 2b).

Under RL, there were no significant differences in Δg_s between the MTs and their WTs and their time courses had almost identical shapes (Fig. 2a, b). Plants of all four genotypes opened their stomata slowly under RL, with Δg_s reaching approximately 90 mmol m^{-2} s^{-1} after one hour of illumination (ZT = 01:00) and remaining at this relatively low value until ZT = 06:00, slowly decreasing thereafter.

Diurnal patterns of A_{net} under BL, GL and RL

The diurnal time-courses of A_{net}, under BL, GL and RL are given in Fig. 2c and d, as curves fitted using linear mixed effect models with 95% confidence bands. The first half hour of data (ZT = 00:00 to 00:30) were culled as the fast increase in A_{net} on illumination could not be adequately captured by recordings at 20 min intervals. After the first half hour of the photoperiod in all light treatments, A_{net} remained stable and no interaction between the three light treatments and genotypes was detected ($p = 0.40$). A_{net} was highest under RL, lower under BL and lowest under GL. The three-way interaction between time (change of A_{net} in time), light treatments and genotypes was significant ($p < 0.0001$). Under BL, GL and RL, A_{net} was no higher in L*er* WT than in Col-5 WT. In both WTs, A_{net} increased slowly during the photoperiod in all light treatments, except under RL where in Col-5 WT A_{net} remained almost constant ($p < 0.0001$). Under BL, A_{net} in *phot1 phot2* tended to be lower than in its WT ($p = 0.074$), while the difference between *cry1 cry2* and its WT was not significant ($p = 0.63$). Under GL, over the day as a whole the MTs did not differ from their respective WTs ($p \geq 0.10$). The slopes over the day of A_{net} differed statistically between MTs and their respective WTs under BL, to a lesser extent GL (both $p < 0.001$), while under RL their slopes were parallel ($p > 0.20$). In spite of their statistical significance relative rates of change in A_{net} were small, ranging between -1.5 % h^{-1} and +2 % h^{-1} over treatments and genotypes (Fig. 2c, d).

Diurnal patterns of Ci/Ca under BL, GL, RL and in darkness

The diurnal patterns of the ratio of intercellular carbon dioxide concentration to ambient carbon dioxide concentration (C_i/C_a) as fitted second degree polynomials and 95% confidence bands are given in Fig. 3. Data from ZT = 00:00 to 00:30 were not included for the same reason as for A_{net}. There were no significant differences in C_i/C_a between genotypes under BL, GL, or RL ($p = 0.54$, SI Script). However, for the photoperiod as a whole, the three-way interaction between light, genotypes and time was significant ($p < 0.0001$, SI Script). The C_i/C_a ratio was lowest under RL, highest in darkness, and similar in BL and GL. Under BL, the ratio initially increased and then decreased from ZT = 06:00 onwards, in all genotypes except in *cry1 cry2* where it remained nearly constant. The ratio of C_i/C_a under RL and GL was similar and slowly decreased towards the end of the photoperiod. In darkness, the ratio was similar between MTs and their WT, slightly above 1.

Diurnal patterns of ΦPSII under BL

We investigated the diurnal patterns of ΦPSII under BL (Fig. 4a, b). ΦPSII in *phot1 phot2* was lower than in its Col-5 WT ($p = 0.008$), decreasing from 16% lower at ZT = 00:30 to a maximum difference of 22% at ZT = 10:00 (Fig 4a). In contrast, the ΦPSII in *cry1 cry2* was similar to its L*er* WT at ZT = 00:30, and differed by a maximum of only 13 % from L*er* at ZT = 10:00 ($p = 0.016$, Fig. 4b).

Rate of increase in Δg_s at the start of illumination under BL, GL and RL

Figure 5 shows fitted third order polynomials for Δg_s with 95% confidence bands for the first hour (ZT = 00:00 to ZT = 01:00) under the light treatments. The model fitted to all the Δg_s data for this period gave significant ($p < 0.001$, SI) two-way and three-way interactions between light colour, genotype and time-of-day. This indicates that the differences between genotypes in the rate of stomatal opening (slope of Δg_s against time) depended on the colour of the light to which the plants were exposed. To identify these patterns, separate statistical analyses were done for each of the light conditions: BL, GL and RL.

Under BL, Δg_s increased at a similar rate in both WTs ($p = 0.072$). While the rate of increase in Δg_s did not differ between *cry1 cry2* and its WT ($p = 0.73$); in *phot1 phot2*, it was less than half that of its WT ($p = 0.002$: Fig. 5). Under GL, there were no differences in Δg_s among the four genotypes during the first hour of illumination ($p = 0.53$). However, under RL, Δg_s differed among genotypes as the result of a slight difference in the shape of the time course during the first hour of illumination in *phot1 phot2* compared to its WT ($p = 0.043$). Furthermore, under RL, the time course of Δg_s was similar in both, *cry1 cry2* compared to its WT ($p = 0.15$), and between the two WTs ($p = 0.15$).

In contrast to the illuminated plants, Δg_s of plants kept in darkness barely changed during the first hour of what would have been the normal photoperiod. They followed the same time-course as during the last hour before ZT = 00:00 with no clear differences between genotypes in the slope of Δg_s against time ($p = 0.03$).

Stomatal density and size

Table 1 presents stomatal density and stomatal size for genotype *cry1 cry2*, its WT L*er*, *phot1 phot2* and its WT Col-5. The slight differences observed between mutants and WTs were not statistically significant (density: abaxial, $p = 0.54$; adaxial, $p = 0.83$; size: abaxial, $p = 0.95$, adaxial, $p = 0.60$, Tab. 1).

Discussion

For half a century, diurnal patterns in g_s have been described using gas-exchange methods (e.g. Tenhunen *et al.* 1987). More recently the use of photoreceptor mutants has improved our understanding of the mechanisms behind stomatal responses to light (e.g. Boccalandro *et al.* 2012). Here, we combined these two approaches to investigate the roles of crys and phots in stomatal opening throughout the day.

The control of diurnal patterns in g_s and A_{net} under BL, GL and RL

Parallel changes in g_s and A_{net} over the diurnal period are ubiquitous because A_{net} depends on CO_2 entering the leaf through stomata. Cowan and Farquhar (1977) were first to consider the theoretical question of what would be the day course of g_s that minimises daily water loss relative to a given level of whole-day carbon assimilation, proposing a model based on an optimization criterion. However, actual measurements of g_s through the day frequently deviate from the predictions of Cowan and Farquhar's (1977) model (Matthews *et al.* 2017).

Regulation of fluxes of CO_2 and water vapour by stomata depends both on functional coupling between g_s and A_{net} and on independent regulation of g_s and A_{net} through parallel responses to the same, or correlated, stimuli (Zeiger *et al*. 1982; Aphalo and Sánchez 1986; Aphalo and Jarvis 1993). Under all three of our11-h constant irradiance treatments (BL, GL, RL), we observed clear diurnal changes in g_s (Figs. 2a, b), while ΦPSII and A_{net} concurrently varied much less (Fig. 2c, d; Fig. 4), which indicates that functional dependence of g_s on A_{net} is unable to fully explain our results. Differences in responses to light of different colours can inform us about the relative importance of functional coupling between g_s and A_{net} *vs.* direct stomatal responses to light (Mansfield and Meidner 1966; Aphalo and Sánchez 1986).

Faster stomatal opening at the beginning of the photoperiod under BL than under RL (Fig. 5) is consistent with the rapid stomatal opening commonly seen in response to acute BL treatments (reviewed by Shimazaki *et al.* 2007). Such direct induction of BL-specific stomatal opening can happen almost immediately, often within seconds of illumination (Zeiger *et al.* 1987; Lawson *et al.* 2010).

The larger Δg_s under BL than under RL throughout the diurnal time-course irrespective of the lower A_{net} and higher C_i (Fig. 2), which might otherwise be expected to negatively regulate Δg_s, indicates that BL-specific maintenance of stomatal opening was active during the whole photoperiod. These results are similar to the gas-exchange time-courses observed in *Xanthium strumarium* by Sharley and Raschke (1981) under BL (peak λ = 455 nm) and RL (λ = 681 nm, applied for 4 h). In this earlier experiment combined RL and BL at 650 µmol m^{-2} s^{-1} photon irradiance gave g_s of 300 mmol m^{-2} s^{-1} after 1 h; g_s remained high at 250 mmol m^{-2} s^{-1} under BL alone, while just RL gave a g_s of only 60 mmol m^{-2} s^{-1}. Given the lower C_i under RL than under BL, the moderately larger Δg_s under RL compared to darkness over the photoperiod could be explained, at least in part, by feedback control on stomatal opening through coupling mediated by C_i depletion.

To a lesser extent than under BL, under GL higher g_s and C_i and lower A_{net} than under RL were maintained throughout the diurnal period, suggesting a contribution from photoreceptors to stomatal opening in GL. Such a role for photoreceptors in GL is consistent with Wang *et al.*'s (2011) observation of A_{net}-independent components in stomatal responses under both BL and GL in sunflower treated with DCMU. Taken together, the different responses we observed under BL, GL and RL indicate that the increase in Δg_s on illumination, and its maintenance throughout the diurnal period, under both BL and GL may partly depend on the BL photoreceptors (discussed next).

The roles of crys and phots in stomatal opening at the start of the day and throughout the photoperiod

The leaf traits of photoreceptor-mutant plants can differ from those of their WT, irrespective of light treatments (Labuz *et al*. 2012; Yu *et al*. 2010). Differences in leaf anatomy, such as in stomatal size and density, can result from the participation of crys in stomatal development (Li

and Yang 2007; Boccalandro *et al.* 2012). However, we found no significant differences between *cry1 cry2* and its L*er* WT in stomatal size or density (Table SI2), which might otherwise have confounded the response of g_s attributable to crys. Differences in light absorptance are dependent on concentration per unit area of chlorophyll and other pigments in leaves which might be modulated through the action of photoreceptors (Hogewoning *et al*. 2010; Thum *et al*. 2001), but these differences were small compared to the responses of Δg_s and $A_{net.}$ in our experiment. Likewise, recordings of g_s before the light treatments and in the darkness treatment (Fig. 1a, b) detected no constitutive differences between the MTs and their respective WTs. Nevertheless, different interactions among photoreceptors are likely to affect responses to full-spectrum solar radiation compared to the monochromatic BL-, RL- and GL treatments employed in our experiments.

The most striking feature differentiating the response of the genotypes under BL was the difference in rate of stomatal opening on illumination (Fig. 5). The rapid stomatal response upon BL illumination we observed in WTs concurs with the findings of Kinoshita *et al*. (2001) that rapid membrane depolarization follows BL illumination (within 30s), which implies that communication between nucleus and plasma membrane is too rapid to implicate changes in gene expression in this response (Shimazaki *et al.* 2007). The lack of a rapid response to BL in the *phot1 phot2* MT agrees with the accepted view for the key role of phots in stomatal opening from experiments of shorter duration than ours (Shimazaki *et al.* 2007). After 2 h 30 min under BL, g_s of *phot1 phot2* was about 50% less than that of its WT Col-5 (ZT > 02:30, Fig. 2a, b), indicating that phots continue to contribute to maintaining g_s after the rapid initial opening. This result concurs with the role of phots in the promotion of continuous stomatal opening through the diurnal period under full sunlight (Boccalandro *et al.* 2012).

Previous studies report that crys can contribute to blue-light-induced stomatal opening under low irradiances (< 100 μmol s^{-1} m^{-2}, Mao *et al.* 2005). However, Boccalandro *et al.* (2012) found crys not to be directly involved in the perception of those signals that promote BL-specific stomatal opening in an experiment under solar radiation (full spectrum). They found that under full sunlight the diurnal patterns of g_s in *cry1 cry2* and *phot1 phot2* had similar shapes to those of their WT, but that *phot1 phot2* had much lower g_s, though both photoreceptors enhanced A_{net}. Our results showed a specific role for crys under BL in the promotion of stomatal opening: following rapid stomatal opening induced by phots, crys were needed for the maintenance of high Δg_s from 2 h 30 min

through the remainder of the photoperiod (ZT > 02:30, Fig. 2a, b). In contrast, A_{net} was comparable in *cry1 cry2* and its WT but C_i was lower in the MT (Figs. 2 and 3), indicating a contribution of crys to stomatal opening mainly independent of A_{net}. It can be speculated that stomatal responses mediated by crys are slower than those mediated by phots because crys' action usually depends on regulation of gene expression (Ohgishi *et al.* 2004).

Interestingly, adding together Δg for the two MTs at each time point throughout the diurnal cycles under BL yields a similar pattern of Δg to that observed in the WTs. This might be interpreted as evidence for an additive effect of phot and cry after 2 h 30 min. This is consistent with Mao *et al.'s* (2005) finding that stomatal aperture in a quadruple MT *cry1 cry2 phot1 phot2* measured on epidermal strips was reduced under 20 μmol s^{-1} m^{-2} BL, compared to that in either of the double MTs *cry1 cry2* or *phot1 phot2*. Further research is needed to better explain how these photoreceptors interact and function together in the control of stomatal opening through the whole diurnal period.

In our experiment, Δg_s was larger under GL than under RL, agreeing with a few reports of stomatal opening driven by GL (Smith *et al*. 2017). Earlier studies did not investigate the involvement of specific photoreceptors in opening of stomata in GL. Consistently with the weak absorption of GL by phots (Christie *et al.* 2015), we found no evidence for a role of phots in stomatal opening in GL. In contrast, Δg_s under GL was smaller in *cry1 cry2* than in its WT (Fig. 2b), with crys accounting for up to 35% of Δg_s 3 h into the photoperiod, indicating a role for them in stomatal opening under GL. This role is consistent with other cry-dependent GL responses and the absorption of GL by light-adapted crys (Folta and Maruhnich 2007; Banerjee *et al.* 2007).

Evidence for crys' involvement in responses of stomata to BL (such as Mao *et al* 2005 and the present study), and in other responses to GL such as shade avoidance (Sellaro *et al.* 2010), de-etiolation (Lin *et al.* 1995) and inhibition of hypocotyl elongation (Ahmad *et al.* 2002), are also consistent with a role for crys in stomatal opening in monochromatic GL. While it has been also observed that GL (540 nm) can antagonise BL-induced stomatal opening (Talbott *et al*. 2002), which is an effect that has been attributed to NPQ1 instead of phots or crys (Talbott *et al*. 2003), our results suggest a positive effect of GL at 516 nm on stomatal opening mediated by crys.

The diurnal course of gas-exchange differs among species (Matthews *et al.* 2017). The differences

are in the speed of stomatal opening at the start of photoperiod and in the later slower increase or decrease in g_s through the rest of the day. Fast opening is important for timely increase in g_s in the morning and in sun flecks (Zeiger *et al.* 1981), improving light utilization for carbon assimilation (Way and Pearcy 2012). Within species, acclimation to different light environments can result in different stomatal opening speeds on exposure to light (Aasamaa and Aphalo 2017; Way and Pearcy 2012). This suggests that separate regulation of opening speed and g_s steady state is possible. The fast phot-dependent response together with the slower cry-dependent BL-specific response could allow such separate regulation of the opening speed and g_s steady-state, providing additional flexibility in the coordination of g_s and A_{net}. As the combined roles of phots and crys in stomatal opening are likely to depend on plants' native habitat and growing conditions, their study will require measurements of whole-day time courses under realistic manipulations and/or simulations of the natural light environment.

Conclusions

We conclude that under an 11 h photoperiod with constant irradiance of 200 μmol m^{-2} s^{-1}: (1) monochromatic BL induces a diurnal pattern of g_s with a broad maximum near ZT = 6:00 to ZT = 7:00 that is different to that under RL or GL; (2) the normal diurnal pattern of g_s in BL requires phots for rapid stomatal opening at the beginning of the photoperiod and both phots and crys afterwards; (3) stomatal opening in GL at 516 nm does not require phots but is likely to partly depend on crys.

Acknowledgments

This research was made possible by funding from the Academy of Finland (decisions 252548 to PJA, and 324555 and 304519 to TMR), China Scholarship Council, The Ella and Georg Ehrnrooth Foundation and Niemi Foundation (to FW). We also thank Dr. Mikael Brosché (University of Helsinki) for seeds of the *cry1 cry2* Arabidopsis mutant.

Conflict of Interest Statement

The authors declare no conflicts of interest

References

Ahmad M, Grancher N, Heil M, Black RC, Giovani B, Galland P, Lardemer D (2002) Action spectrum for cryptochrome-dependent hypocotyl growth inhibition in Arabidopsis. *Plant Physiology* **129**, 774–785.

Ando E, Ohnishi M, Wang Y, Matsushita T, Watanabe A, Hayashi Y, Fujii M, Ma JF, Inoue S-I, Kinoshita T (2013) TWIN SISTER OF FT, GIGANTEA, and CONSTANS have a positive but indirect effect on blue light-induced stomatal opening in Arabidopsis. *Plant Physiology* **162**, 1529–1538.

Aphalo PJ (2015) The r4photobiology suite: spectral irradiance. *UV4Plants Bulletin* **2015**, 21–29.

Aphalo PJ, Jarvis PG (1993) Separation of Direct and Indirect Responses of Stomata to Light - Results From a Leaf Inversion Experiment at Constant Intercellular CO_2 Molar Fraction. *Journal of experimental botany* **44**,791–800.

Aphalo PJ, Sánchez RA (1986) Stomatal Responses to Light and Drought Stress in Variegated Leaves of Hedera helix. *Plant Physiology* **81**,768–773

Aasamaa K, Aphalo PJ (2017) The acclimation of *Tilia cordata* stomatal opening in response to light, and stomatal anatomy to vegetational shade and its components. Tree Physiology **37**, 209–219

Banerjee R, Batschauer A (2005) Plant blue-light receptors. *Planta* **220**, 498–502.

Banerjee R, Schleicher E, Meier S, Viana RM (2007) The signaling state of Arabidopsis cryptochrome 2 contains flavin semiquinone. *Journal of Biological Chemistry* **282**,14916–14922.

Boccalandro HE, Giordano CV, Ploschuk EL, Piccoli PN, Bottini R, Casal JJ (2012) Phototropins But Not Cryptochromes Mediate the Blue Light-Specific Promotion of Stomatal Conductance, While Both Enhance Photosynthesis and Transpiration under Full Sunlight. *Plant Physiology* **158**, 1475–1484.

557 Briggs WR, Huala E (1999) Blue-light photoreceptors in higher plants. *Annual review of cell and*
558 *developmental biology* **15**, 33–62.

559 Chen C, Xiao Y, Li X, Ni M (2012) Light-Regulated Stomatal Aperture in Arabidopsis.
560 *Molecular plant* **5**, 566–572.

561 Christie JM (2007) Phototropin blue-light receptors. *Annual Review of Plant Biology* **58**, 21–45.

562 Christie JM, Blackwood L, Petersen J, Sullivan S (2015) Plant flavoprotein photoreceptors. *Plant*
563 *and Cell Physiology* **56**, 401–413.

564 Cowan IR, Farquhar GD (1977) Stomatal function in relation to leaf metabolism and
565 environment. *Symposia of the Society for Experimental Biology* **31**, 471–505.

566 de Dios VR, Gessler A, Ferrio JP, Alday JG, Bahn M, del Castillo J, Devidal S, García-Muñoz S,
567 Kayler Z, Landais D, Martín-Gómez P, Milcu A, Piel C, Pirhofer-Walzl K, Ravel O, Salekin
568 S, Tissue DT, Tjoelker MG, Voltas J, Roy J (2016) Circadian rhythms have significant
569 effects on leaf-to-canopy scale gas exchange under field conditions. *GigaScience* **5**, 1-10

570 Inoue S-I, Takemiya A, Shimazaki K-I (2010) Phototropin signaling and stomatal opening as a
571 model case. *Current Opinion in Plant Biology* **13**, 587–593.

572 Folta KM, Maruhnich SA (2007) Green light: a signal to slow down or stop. *Journal of*
573 *experimental botany* **58**, 3099–3111.

574 Frechilla S, Talbott LD, Bogomolni RA, Zeiger E (2000) Reversal of Blue Light-Stimulated
575 Stomatal Opening by Green Light. *Plant and Cell Physiology* **41**, 171–176.

576 Genty B, Briantais J-M, Baker NR (1989) The relationship between the quantum yield of
577 photosynthetic electron transport and quenching of chlorophyll fluorescence. *Biochimica Et*
578 *Biophysica Acta (BBA) - General Subjects* **990**, 87–92.

579 Hogewoning SW, Trouwborst G, Maljaars H, POORTER H, van Ieperen W, Harbinson J (2010)
580 Blue light dose-responses of leaf photosynthesis, morphology, and chemical composition of
581 *Cucumis sativus* grown under different combinations of red and blue light. *Journal of*

Experimental Botany **61**, 3107–3117.

Kinoshita T, Doi M, Suetsugu N, Kagawa T, Wada M, Shimazaki K (2001) Phot1 and phot2 mediate blue light regulation of stomatal opening. *Nature* **414**, 656–660.

Kinoshita T, Ono N, Hayashi Y, Morimoto S, Nakamura S, Soda M, Kato Y, Ohnishi M, Nakano T, Inoue S-I, Shimazaki K-I (2011) FLOWERING LOCUS T Regulates Stomatal Opening. *Current Biology* **21**, 1232–1238.

Labuz J, Sztatelman O, Banas AK, Gabrys H (2012) The expression of phototropins in Arabidopsis leaves: developmental and light regulation. *Journal of Experimental Botany* **63**, 1763–1771.

Lawson T, Caemmerer von S, Baroli I (2010) Photosynthesis and Stomatal Behaviour. pp. 265–304 in *Progress in Botany Springer* Berlin Heidelberg: Berlin, Heidelberg.

Li Q-H, Yang H-Q (2007) Cryptochrome signaling in plants. *Photochemistry and Photobiology* **83**, 94–101.

Lin C, Ahmad M, Gordon D, Cashmore AR (1995) Expression of an Arabidopsis cryptochrome gene in transgenic tobacco results in hypersensitivity to blue, UV-A, and green light. *Proceedings of the National Academy of Sciences* **92**, 8423–8427.

Liscum E, Hodgson DW, Campbell TJ (2003) Blue light signaling through the cryptochromes and phototropins. So that's what the blues is all about. *Plant Physiology* **133**, 1429–1436.

Mao J, Zhang Y-C, Sang Y, Li Q-H, Yang H-Q (2005) From The Cover: A role for Arabidopsis cryptochromes and COP1 in the regulation of stomatal opening. *Proceedings of the National Academy of Sciences* **102**, 12270–12275.

Matthews JSA, Vialet-Chabrand SRM, Lawson T (2017) Diurnal Variation in Gas Exchange: The Balance between Carbon Fixation and Water Loss. *Plant Physiology* **174,** 614–623

Ohgishi M, Saji K, Okada K, Sakai T (2004) Functional analysis of each blue light receptor, cry1, cry2, phot1, and phot2, by using combinatorial multiple mutants in Arabidopsis.

Proceedings of the National Academy of Sciences **101**, 2223–2228.

Pinheiro JC, Bates DM (2000) Nonlinear Mixed-Effects Models: Basic Concepts and Motivating Examples pp. 273–304 in *Mixed-Effects Models in Sand S-PLUS*. Statistics and Computing. Springer New York: New York, NY.

R Core Team (2016) R: A Language and Environment for Statistical Computing. Vienna, Austria.

Roelfsema MRG, Hanstein S, Felle HH, Hedrich R (2002) CO_2 provides an intermediate link in the red light response of guard cells. *The Plant Journal* **32**, 65–75.

Saw NMMT, Moser C, Martens S, Franceschi P (2017) Applying generalized additive models to unravel dynamic changes in anthocyanin biosynthesis in methyl jasmonate elicited grapevine (*Vitis vinifera* cv. Gamay) cell cultures. *Horticulture Research* **4**, 17038.

Sellaro R, Crepy M, Trupkin SA, Karayekov E, Buchovsky AS, Rossi C, Casal JJ (2010) Cryptochrome as a sensor of the blue/green ratio of natural radiation in Arabidopsis. *Plant Physiology* **154**, 401–409.

Sellaro R, Pacín M, Casal JJ (2012) Diurnal dependence of growth responses to shade in Arabidopsis: role of hormone, clock, and light signaling. *Molecular plant* **5**, 619–628.

Sharkey TD, Raschke K (1981) Effect of Light Quality on Stomatal Opening in Leaves of *Xanthium strumarium* L. *Plant Physiology* **68**, 1170–1174.

Sharkey TD, Ogawa T (1987) Stomatal responses to light pp. 195-208 in *Stomatal function*. (ed. Zeiger E, Farquhar GD, Cowan IR) Stanford University Press

Shimazaki K-I, Doi M, Assmann SM, Kinoshita T (2007) Light Regulation of Stomatal Movement. *Annual Review of Plant Biology* **58**, 219–247.

Smith HL, McAusland L, Murchie EH (2017) Don't ignore the green light: exploring diverse roles in plant processes. *Journal of experimental botany* **68**, 2099–2110.

Talbott LD, Zeiger E (1996) Central Roles for Potassium and Sucrose in Guard-Cell

632 Osmoregulation. *Plant Physiology* **111**, 1051–1057.

633 Talbott LD, Nikolova G, Ortiz A, Shmayevich I, Zeiger E (2002) Green light reversal of blue-
634 light-stimulated stomatal opening is found in a diversity of plant species. *American Journal*
635 *of Botany* **89**, 366–368.

636 Talbott LD, Shmayevich IJ, Chung Y, Hammad JW, Zeiger E (2003) Blue light and
637 phytochrome-mediated stomatal opening in the *npq1* and *phot1 phot2* mutants of
638 Arabidopsis. *Plant Physiology* **133**, 1522–1529.

639 Tallman G (2004) Are diurnal patterns of stomatal movement the result of alternating
640 metabolism of endogenous guard cell ABA and accumulation of ABA delivered to the
641 apoplast around guard cells by transpiration? *Journal of experimental botany* **55**, 1963–1976.

642 Tenhunen JD, Pearcy RW, Lange OL (1987) Diurnal Variations in Leaf Conductance and Gas
643 Exchange in Natural Environments. (eds. E Zeiger, GD Farquhar and IR Cowan) *Stomatal*
644 *function*. Stanford University Press, 323-351

645 Thum KE, Kim M, Christopher DA, Mullet JE (2001) Cryptochrome 1, cryptochrome 2, and
646 phytochrome a co-activate the chloroplast *psbD* blue light-responsive promoter. *The Plant*
647 *Cell Online* **13**, 2747–2760.

648 Yu X, Liu H, Klejnot J, Lin C (2010) The Cryptochrome Blue Light Receptors. *The Arabidopsis*
649 *Book* **8**, e0135.

650 Wang F (2017) Tutorial: SIOX plugin in ImageJ: area measurement made easy. *UVPlants*
651 *Bulletin* **2**.

652 Wang Y, Noguchi K, Terashima I (2011) Photosynthesis-dependent and -independent responses
653 of stomata to blue, red and green monochromatic light: differences between the normally
654 oriented and inverted leaves of sunflower. *Plant and Cell Physiology* **52**, 479–489.

655 Way DA, Pearcy RW (2012) Sunflecks in trees and forests: from photosynthetic physiology to
656 global change biology. *Tree Physiology* **32**, 1066–1081.

Wood S (2006) Generalized Additive Models: an introduction with R. CRC Press

Zeiger E, Field C (1982) Photocontrol of the Functional Coupling between Photosynthesis and Stomatal Conductance in the Intact Leaf : Blue Light and Par-Dependent Photosystems in Guard Cells. *Plant Physiology* **70**, 370–375.

Zeiger E, Field C, Mooney HA (1981) Stomatal opening at dawn: possible roles of the blue light response in nature in *Plants and the Daylight Spectrum*. Academic Press. 391-407

Zeiger E, Iino M, Shimazaki K-I, Ogawa T (1987) The blue-light response of stomata. In Stomatal function. Stanford University Press. 209-227

Figure legends

Fig. 1. Time courses of gas-exchange between ZT = 00:00 and ZT = 11:30 in darkness in *phot1 phot2* (---), its WT Col-5 (—), *cry1 cry2* (---) and its WT L*er* (—). (a, b) Change in stomatal conductance (Δg_s) from ZT = 00:00; (c, d) Net carbon assimilation rate (A_{net}). Negative net carbon assimilation rate in darkness is respiration. Lines depict prediction by a fitted additive mixed models (AMM) (a, b) and mixed-effect linear models (c, d); grey bands depict 95% confidence limits; n = 3 – 4 plants per genotype, N = 14 plants, 1040 observations in total. The vertical dashed lines highlight ZT = 00:00, the time when LEDs were switched on during gas-exchange measurements for treatments not remaining in darkness.

Fig. 2 Time courses of gas-exchange between ZT = 00:00 and ZT = 11:30 under constant irradiance of BL, GL, or RL in *phot1 phot2* (---), its WT Col-5 (—), *cry1 cry2* (---) and its WT L*er* (—). (a, b) Change in stomatal conductance (Δg_s) from ZT = 00:00; (c, d) Net carbon assimilation rate (A_{net}). Lines depict prediction by a fitted additive mixed models (AMM) (a, b) and mixed effects model based on mixed-effect linear models (c, d) ; grey bands depict 95% confidence limits; n = 3 – 4 plants per light colour and genotype, N = 44 plants, 3371 observations in total. The vertical dashed lines highlight ZT = 00:00, the time when LEDs were switched on during gas-exchange measurements, except for plants remaining in darkness. Equivalent figures showing raw g_s and A_{net} data are presented in Figs. SI 4 and 5 respectively.

Fig. 3 Ratio of intercellular and ambient carbon dioxide (C_i/C_a) in *phot1 phot2* (---) and its WT Col-5 (—) under constant irradiance of BL (a), GL (b), RL (c) and in darkness (d), and in *cry1 cry2* (---) and its WT L*er* (—) under BL (e), GL (f), RL (g) and in darkness (h) between ZT = 00:30 and ZT = 11:30. Lines depict prediction by a fitted mixed effects model based on linear models and grey bands depict 95% confidence limits, n = 3 – 4 plants per light colour and genotype, N = 44 plants, 4262 observations in total. The vertical dashed lines highlight ZT = 00:00, the time when LEDs were switched on during gas-exchange measurements, except for plants remaining in darkness. The C_a is given in Table SI1.

Fig. 4 Effective photochemical quantum yield of photosystem PSII photochemistry (ΦPSII) under constant irradiance of BL between ZT = 00:30 and ZT = 11:30 in *phot1 phot2* (---) and its WT Col-5 (—) (a) and in *cry1 cry2* (---) and its WT L*er* (—) (b). Lines depict prediction by a fitted mixed effects model based on linear models and grey bands depict 95% confidence limits,

n = 4 plants per light colour and genotype, N = 62 plants, 3828 observations in total. The vertical dashed lines highlight ZT = 00:00, the time when LEDs were switched on during gas-exchange measurements, except for plants remaining in darkness.

Fig. 5 Change in stomatal conductance (Δg_s) in *phot1 phot2* (---) and its WT Col-5 (—) under constant irradiance of BL (a), GL (b), RL (c) and in darkness (d), and in *cry1 cry2* (---) and its WT L*er* (—) under BL (e), GL (f), RL (g) and in darkness (h) between ZT = 00:00 and ZT = 01:00. Lines depict prediction by a fitted mixed effects model based on third-order polynomials and grey bands depict 95% confidence limits, n = 3 – 4 plants per light colour and genotype, N = 58 plants, 340 observations in total. Data of g_s for individual plants are given in Fig. SI4. The vertical dashed lines highlight ZT = 00:00, the time when LEDs were switched on during gas-exchange measurements, except for plants remaining in darkness

Legends to supplemental figures

Fig. SI1 Spectral photon irradiance measured in the growth room with a cosine diffuser level with the top of the seedlings. Spectral irradiance on the growth room shelves was measured with a Maya2000 Pro spectrometer (Ocean Optics, U.S.A) fitted with a D7-H-SMA cosine diffuser (Bentham Instruments, Reading, U.K.).

Fig. SI2a Normalized spectral photon irradiance of (non-polarized) light emitted by the red, green, and blue channels of the LED-array source used for gas-exchange measurements (presented in Fig SI3, SI4 and SI5). The overlap in normalized photon irradiance between the blue and green channels is 3.9% of their combined photon irradiance, and between green and red channels the overlap is 0.4%. There is no measurable overlap (<0.05%) between red and blue channels; SI2b Photograph of the custom-built LED-array light source used for gas-exchange measurements. Each array has three independent channels, emitting BL, GL, or RL.

Fig. SI3 Stomatal conductance (g_s) for individual plants from 12 midnight until 6 p.m. on the next day. These data were used to calculate the Δg_s values used in the model fits presented in Figs. 2 and 3, and in statistical tests of significance. The vertical dashed lines highlight 7 a.m. local time (ZT = 00:00), the time when LEDs were switched on during gas-exchange measurements, except for plants remaining in darkness.

Fig. SI4 Net carbon assimilation rate (A_{net}) for individual plants from 12 midnight until 6 p.m. on the next day. These data were used to calculate A_{net} values used in the model fits presented in Figs. 2 and 3, and in statistical tests of significance. Negative net carbon assimilation rate in darkness is respiration. The vertical dashed lines highlight 7 a.m. local time (ZT = 00:00), the time when LEDs were switched on during gas-exchange measurements, except for plants remaining in darkness.

Fig. SI5 Ratio of C_i/C_a for individual plants from 12 midnight until 6 p.m. on the next day. These data were used to calculate ratio of C_i/C_a values used in the model fits presented in Figs. 4, and in statistical tests of significance. The vertical dashed lines highlight 7 a.m. local time (ZT = 00:00), the time when LEDs were switched on during gas-exchange measurements, except for plants remaining in darkness. Concentrations of C_a are listed in Table SI1.

Fig. SI6 Light absorption. Average spectral absorptance of illuminated leaves from 5 or 6 plants of each genotype. Upper panel: The colour bars show the full width at half maximum (FWHM) of the peak of photon emission spectra of the three LED channels from Fig. SI2a. Lower panel: Estimate of the photon dose rate computed as the absorbed irradiance by convolution of the absorptance spectra of the leaves (upper panel) with the emission spectra of the LEDs (Fig. SI2a) integrated over wavelengths. The dashed line indicates the photon irradiance incident on the plants. The absorbed energy irradiances averaged over genotypes were: RL 34.3 W m^{-2}, GL 41.4 W m^{-2}, and BL 50.4 W m^{-2}.

Tables

Table 1. Stomatal size and density, mean ± SE, n = 10. Size is expressed as the maximum length of the guard cells along the length of the pore; density is expressed as number of stomata per unit leaf area.

Genotype	Epidermis	Size (μm)	Density (mm^{-2})
Col-5	Adaxial	18.6 ± 0.4	163 ± 11
	Abaxial	19.2 ± 1.4	191 ± 16
phot1 phot2	Adaxial	18.6 ± 0.4	142 ± 32
	Abaxial	19.2 ± 1.4	184 ± 28
L*er*	Adaxial	20.3 ± 0.8	164 ± 27
	Abaxial	19.0 ± 1.0	171 ± 17
cry1 cry2	Adaxial	18.8 ± 0.5	150 ± 17
	Abaxial	19.0 ± 1.0	146 ± 18

Table SI1. Concentration of C_a maintained by gas-exchange system under each light treatment for each genotype during the period of ZT = 00:00 to ZT = 11:30.

	Red light	Green light	Blue light	Darkness
Col-5	387.6 ± 0.1	387.8 ± 0.1	387.6 ± 0.1	390.3 ± 0.0
phot1 phot2	388.4 ± 0.0	388.1 ± 0.1	388.4 ± 0.1	390.3 ± 0.0
L*er*	386.9 ± 0.1	387.4 ± 0.1	386.9 ± 0.1	390.1 ± 0.0
cry1 cry2	387.8 ± 0.1	387.9 ± 0.1	387.8 ± 0.1	390.1 ± 0.0

754 Fig. 1

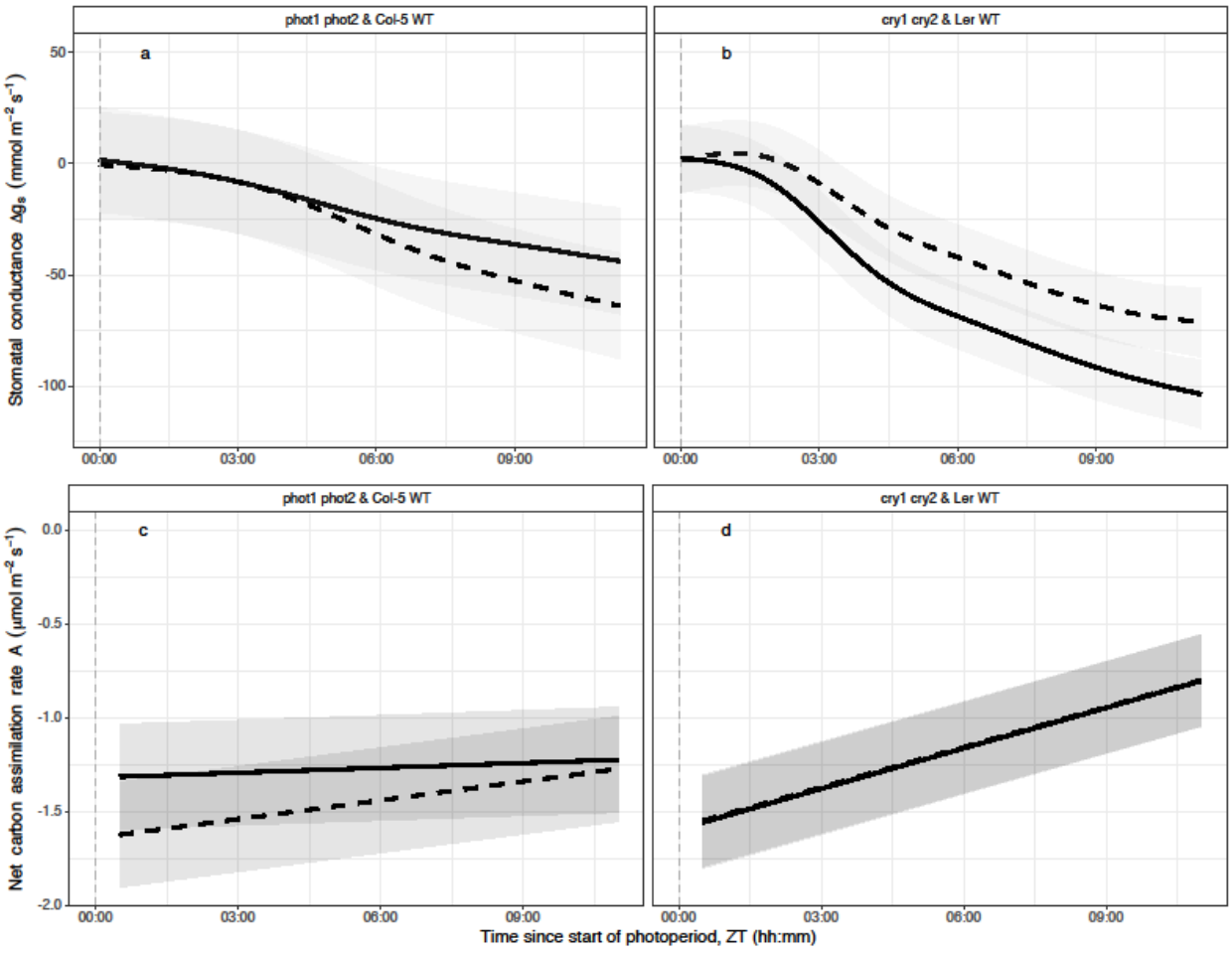
phot1 phot2 & Col-5 WT
cry1 cry2 & Ler WT
a
b
c
d
Stomatal conductance Δgs (mmol m-2 s-1)
Net carbon assimilation rate A (μmol m-2 s-1)
50
0
-50
-100
0.0
-0.5
-1.0
-1.5
-2.0
00:00
03:00
06:00
09:00
Time since start of photoperiod, ZT (hh:mm)

755

Fig. 2

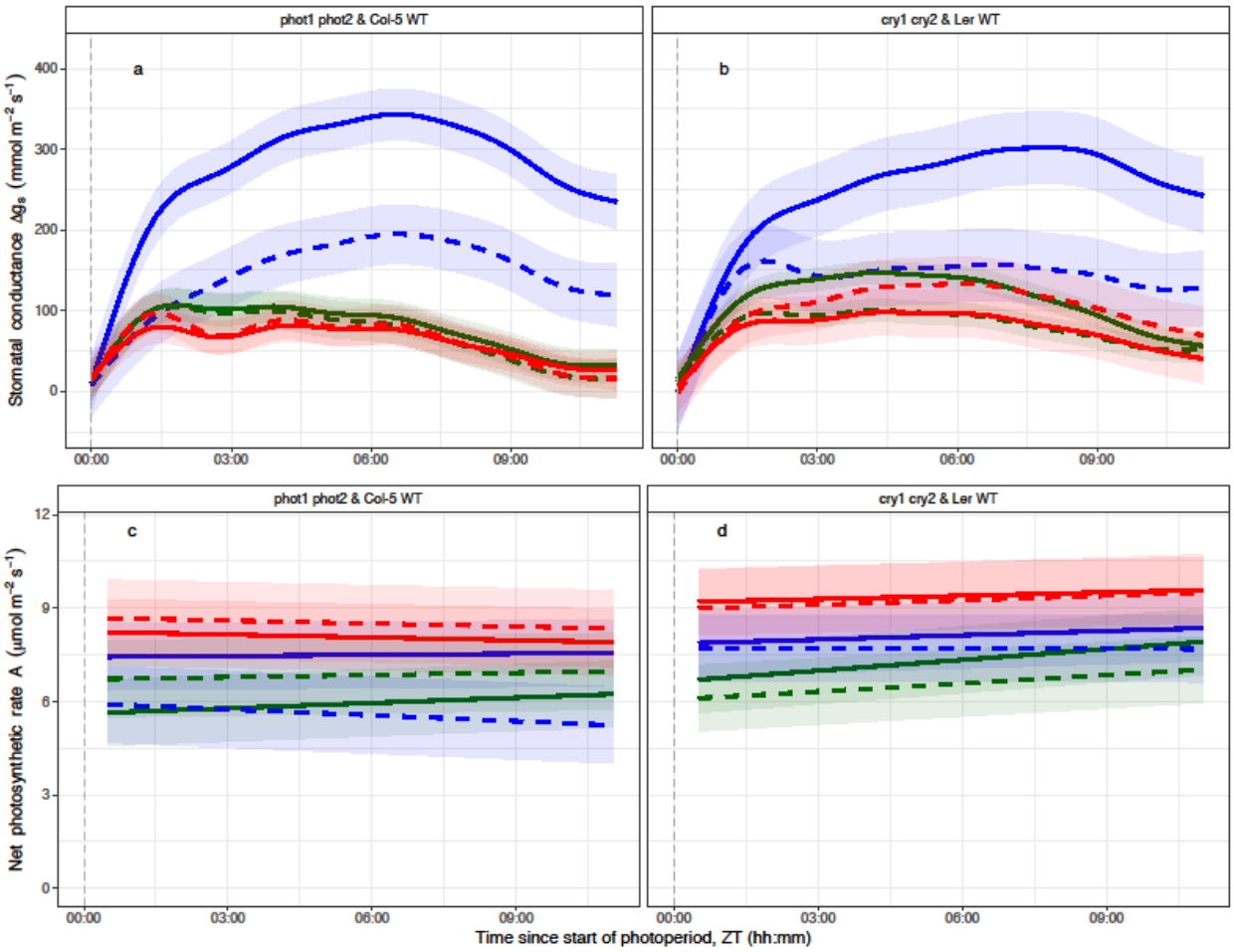
phot1 phot2 & Col-5 WT
cry1 cry2 & Ler WT
a
b
c
d
Stomatal conductance Δg_s (mmol m^{-2} s^{-1})
Net photosynthetic rate A (µmol m^{-2} s^{-1})
0
100
200
300
400
0
3
6
9
12
00:00
03:00
06:00
09:00
Time since start of photoperiod, ZT (hh:mm)

758 Fig. 3

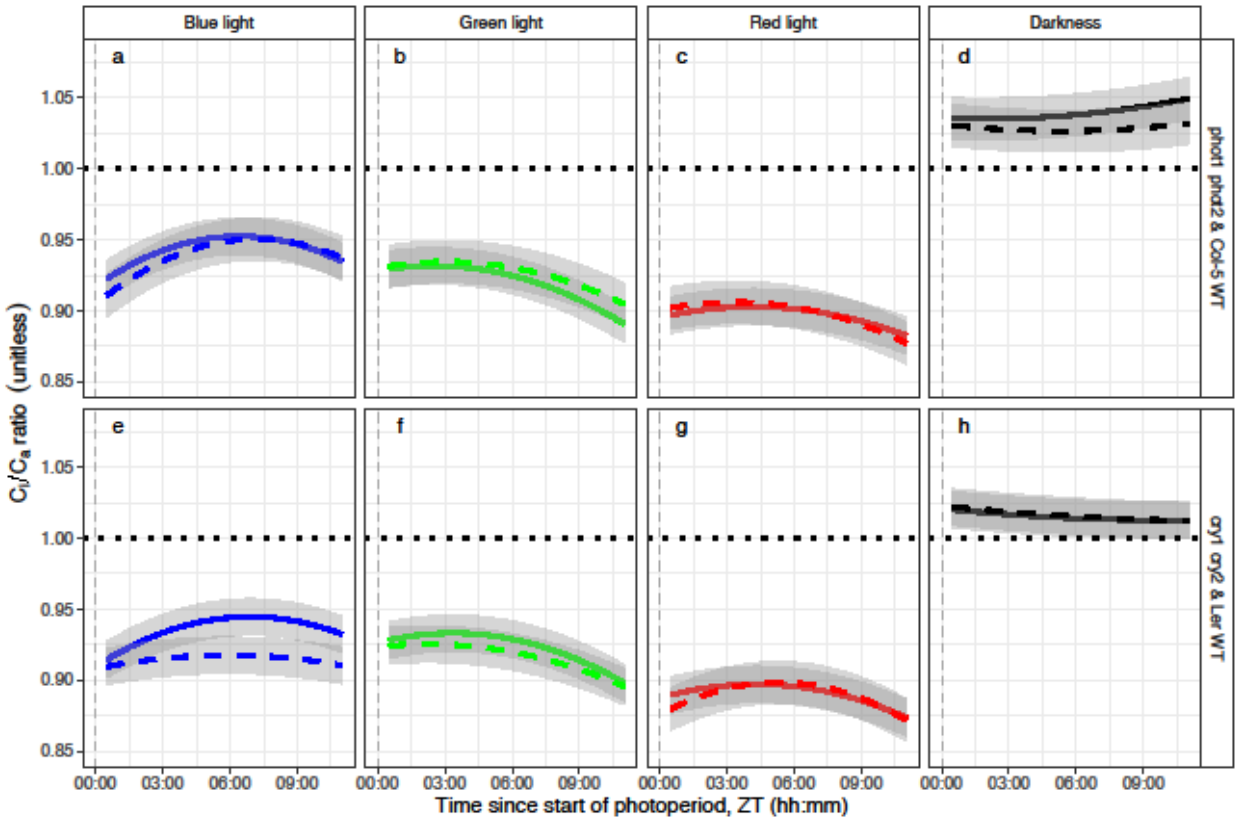
Blue light
Green light
Red light
Darkness
a
b
c
d
e
f
g
h
phot1 phot2 & Col-5 WT
cry1 cry2 & Ler WT
C_i/C_a ratio (unitless)
1.05
1.00
0.95
0.90
0.85
00:00
03:00
06:00
09:00
Time since start of photoperiod, ZT (hh:mm)

759

760 Fig. 4

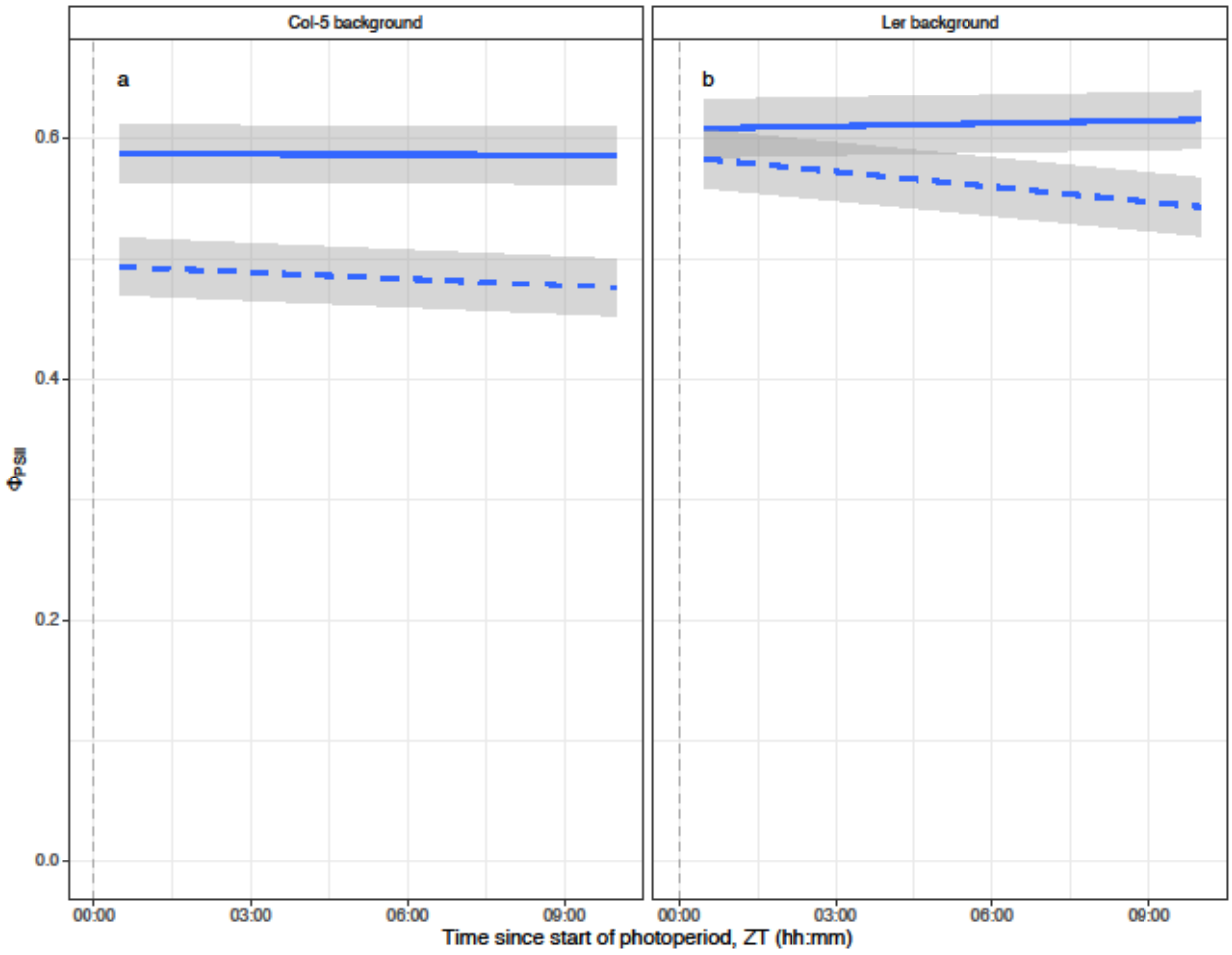
Col-5 background
Ler background
a
b
0.6
0.4
0.2
0.0
ΦPSII
00:00
03:00
06:00
09:00
Time since start of photoperiod, ZT (hh:mm)

761

762 Fig. 5

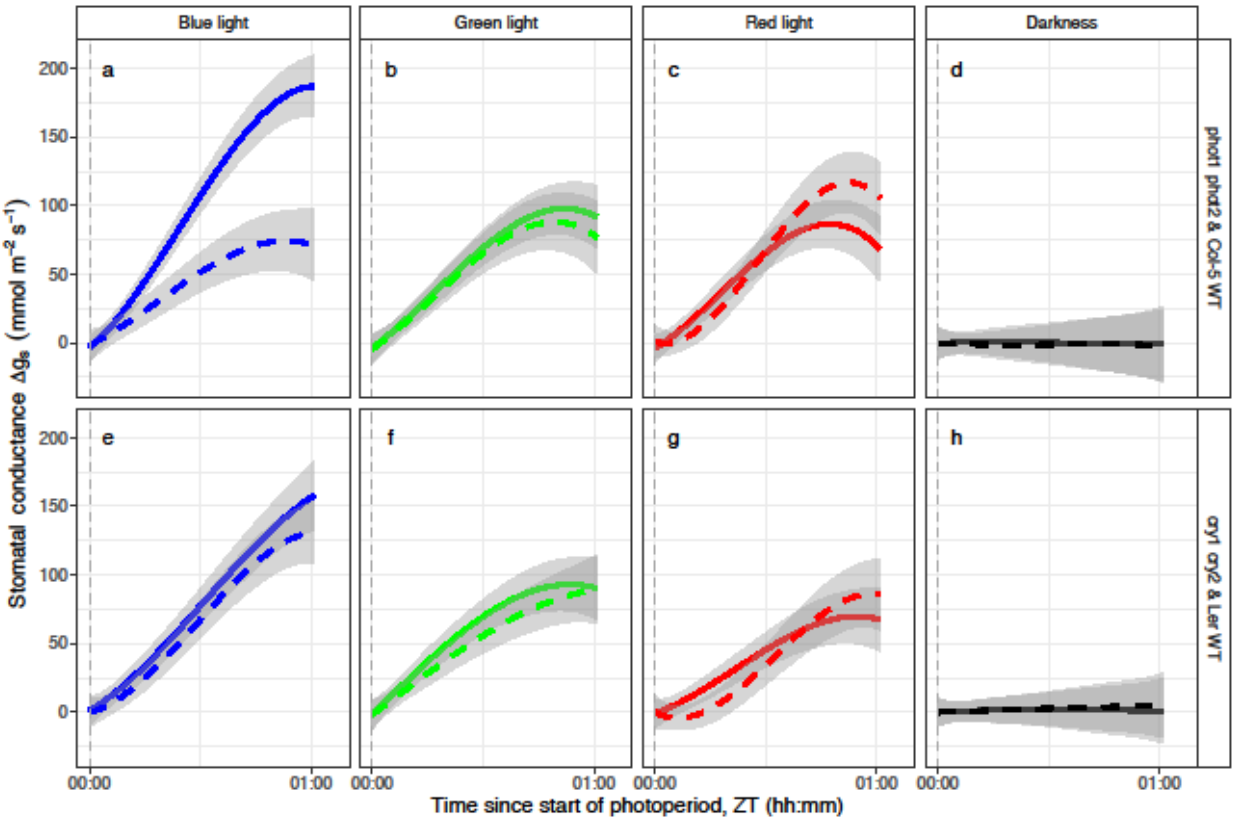
Blue light
Green light
Red light
Darkness
a
b
c
d
e
f
g
h
phot1 phot2 & Col-5 WT
cry1 cry2 & Ler WT
Stomatal conductance Δgs (mmol m-2 s-1)
200
150
100
50
0
00:00
01:00
Time since start of photoperiod, ZT (hh:mm)

763